On the mechanism of the [4+2] cycloaddition of $^1O_2$ with 1,3-dienes: Identifying the putative biradical/dipolar intermediate by employing the *gem*-diphenylcyclopropylcarbinyl radical clock as a mechanistic probe

Manolis D. Tzirakis[a,b] and Mariza N. Alberti[a]*

[a] *Department of Chemistry, University of Crete, Voutes Campus, GR-71003, Heraklion, Crete, Greece*
[b] *Current address: Institute of Chemistry and Biological Chemistry, Zurich University of Applied Sciences, Einsiedlerstrasse 31, CH-8820, Wädenswil, Switzerland*
E-mail: *alberti@chemistry.uoc.gr*

This paper is dedicated to our mentor, Prof. Michael Orfanopoulos, on the occasion of his 67th birthday, and his outstanding contribution to singlet oxygen and fullerene chemistry

Abstract

The mechanism of the [4+2] cycloaddition reaction of singlet oxygen ($^1O_2$) with simple acyclic dienes, *i.e.* (*E*)/(*Z*)-**1** and (*E,E*)/(*Z,E*)-**2**, was investigated by employing the *gem*-diphenylcyclopropylcarbinyl radical clock as a hypersensitive mechanistic probe. In both cases, benzophenone, a decomposition product of the rearranged endoperoxide intermediates **11** and **12**, was identified as the major product. The formation of this product is consistent with the intervention of an open biradical or dipolar intermediate having a lifetime greater than 2 psec. Our attempts to further trap any endoperoxide intermediate revealed a new mode of reactivity of these dienic systems with $^3O_2$, that mainly affords the corresponding 1,2-dioxolane derivatives (*E*)-**13** and (*E,E*)-**14**, respectively, through a photoinduced electron transfer mechanism, co-sensitized by methylene blue (MB) and thiourea. The structures of (*E*)-**13** and (*E,E*)-**14** were supported by experimental and theoretical NMR studies.

Keywords: [4+2] Cycloaddition, 1,3-dienes, cyclopropyl probes, singlet oxygen, 1,2-dioxolanes, reaction mechanisms

Introduction

Reactions of singlet oxygen ($^1O_2$), the common name used for the diamagnetic, first excited state of molecular oxygen ($^3O_2$),[1–3] play a key role in many diverse fields, ranging from atmospheric chemistry and materials science to biology and medicine.[4,5] In particular, $^1O_2$ plays a key role as a synthetic reagent for the synthesis of fine chemicals,[1–3,6] as intermediate in oxygenation reactions of polymers,[7] in the treatment of wastewater,[8,9] as a non-radical reactive oxygen species (ROS) which is closely associated with tissue damage and various diseases,[10–12] and also in photodynamic applications such as blood sterilization, sunlight-activated herbicides and insecticides, and photodynamic therapy (PDT) of cancer.[4,5,13,14] Among the various types of $^1O_2$ reactions, the [4+2] cycloaddition of $^1O_2$ has inevitably drawn great attention, and compounds embodying the endoperoxide functional group are prevalent throughout chemistry.[15–17] Several theoretical and experimental studies have been performed in the past to unravel the mechanistic details in the [4+2] cycloaddition of $^1O_2$ with cyclic or acyclic 1,3-dienes, and aromatic or heteroaromatic compounds.[18–22] Overall, there are two general mechanistic pathways that have been proposed for this reaction, which, in particular, include a concerted and a stepwise pathway. In the first pathway, the formation of the [4+2] cycloadduct proceeds in a concerted fashion *via* either a symmetrical (Scheme 1, pathway A) or an unsymmetrical (Scheme 1, pathway B) transition state.[22–28] On the other hand, the second pathway proceeds in a stepwise fashion, that involves the intervention of a peroxirane (perepoxide; Scheme 1, pathway C),[29] a zwitterionic (Scheme 1, pathway D) or a biradical (Scheme 1, pathway E) intermediate.[22,27,30–32] It has been further proposed that the reversible formation of an exciplex (Scheme 1, pathway F) precedes product formation.[18,30,33–35] Typically, the mechanism of the [4+2] cycloaddition of $^1O_2$ with unsaturated substrates does not follow a general scheme and is highly sensitive to both the substrate structure and the reaction conditions. For example, 1,3-dienes in which the 2,3-single bond is not flexible, the [4+2] cycloaddition with $^1O_2$ is stereoselective, while 1,3-dienes that bear a flexible 2,3-single bond may react with $^1O_2$ *via* a biradical or dipolar intermediate which, in turn, may collapse to products or revert to the initial dienes with concomitant *cis-trans* isomerism.[31] Foote and O'Shea have previously reported the trapping of such intermediates, particularly zwitterionic intermediates, in the [4+2] cycloaddition of $^1O_2$ with simple dienes (*i.e.* 2,4-hexadienes) in MeOH.[31] Nevertheless, despite the large number of related mechanistic studies, the trapping of such biradical or dipolar intermediates has not been observed in nonpolar solvents.
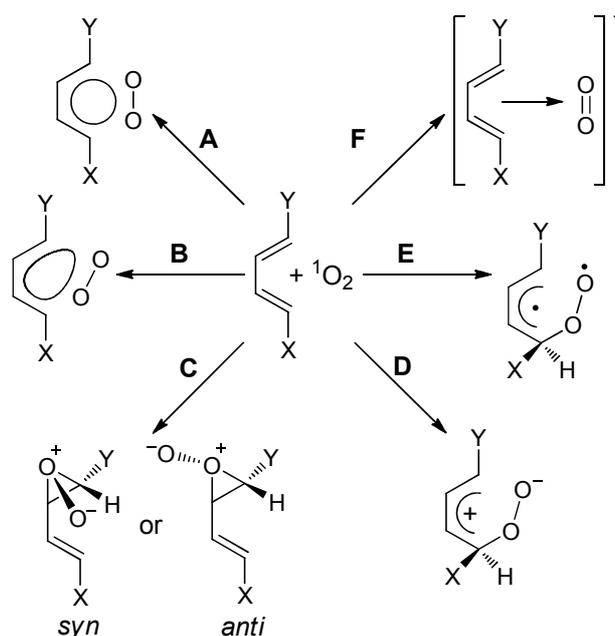
Scheme 1. Possible transition states or reaction intermediates proposed for the [4+2] cycloaddition of $^1O_2$ with cyclic or acyclic 1,3-dienes.

The present study was undertaken with the goal to provide insight into the [4+2] cycloaddition reaction mechanism of $^1O_2$ with acyclic 1,3-dienes and, in particular, to ascertain precisely the possible involvement of an open biradical/dipolar intermediate. For this purpose, we used highly informative substrates, *i.e.* 1,3-dienes (*E*)/(*Z*)-**1** and (*E,E*)/(*Z,E*)-**2**, which bear the *gem*-diphenylcyclopropyl group as a hypersensitive mechanistic probe (Scheme 2a). Substituted cyclopropyl groups have been used as traps for other radical intermediates,[36–39] since they involve the rapid ring opening of the cyclopropylcarbinyl radical to the corresponding homo-allylcarbinyl radical.[40] For example, Newcomb and co-workers reported that *gem*-diphenylcyclo-propylcarbinyl radical **3** rearranges rapidly to the corresponding homoallylcarbinyl radical **4** with experimental rate constant of 5×10^{11} s^{-1} at 25 ^{o}C (Scheme 2b).[41] This probe is often used as a *radical clock* to quantify a radical lifetime.[42] The synthesis of (*E*)/(*Z*)-**1** and (*E,E*)/(*Z,E*)-**2** was described in a previous work.[39] As compared to (*E*)/(*Z*)-**1**, the less-substituted diene (*E,E*)/(*Z,E*)-**2** bears one alkyl substituent on each double bond carbon C(1) and C(4), correspondingly, thus rendering both double bonds almost electronically equivalent and therefore equally competitive for the $^1O_2$ addition. In the case of an open biradical/dipolar intermediate, a secondary radical/carbocation in both C(1) and C(4) carbons may be formed, thus leading to products derived from both sides of the diene moiety.

(a)

$(E)/(Z)$-**1** $(E,E)/(Z,E)$-**2**
$(E/Z = 30/70)$ $(E,E/Z,E = 35/65)$

(b)

k_r (25 ^{o}C) = 5 × 10^{11} s^{-1}

3   **4**
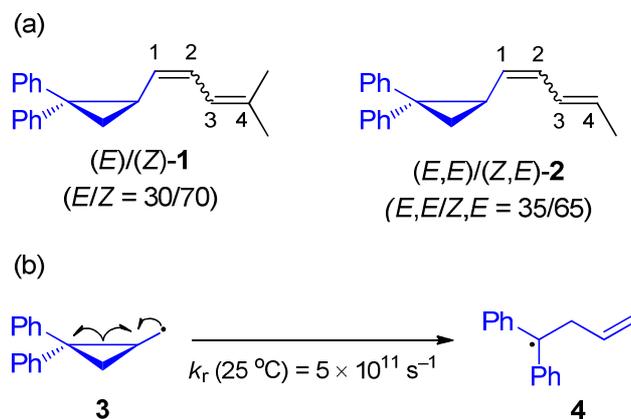
Scheme 2. (a) Structures of *gem*-diphenylcyclopropyl-substituted 1,3-dienes $(E)/(Z)$-**1** and $(E,E)/(Z,E)$-**2**,[43] showing the numbering system adopted in the present work for identifying their relevant vinyl-C-atoms discussed in the text. (b) Rearrangement of the *gem*-diphenylcyclo-propylcarbinyl radical **3** to the corresponding homoallylcarbinyl radical **4**. The *gem*-diphenyl-cyclopropylcarbinyl radical clock is highlighted in blue.

Results and Discussion

Endoperoxides are usually highly reactive compounds, which prompted us to perform the photooxygenation of $(E)/(Z)$-**1** and $(E,E)/(Z,E)$-**2** under mild conditions of relatively low temperatures (*i.e.* –78, –40 and 0 ^{o}C) in oxygen-saturated CCl$_4$, CH$_2$Cl$_2$, CH$_3$CN, or MeOH. Previous studies have shown that the use of CCl$_4$ as the reaction solvent favors the formation of the [4+2] cycloaddition product over the products derived from other ^{1}O$_2$ reaction modes (*i.e.* 'ene' reaction or [2+2] cycloaddition).[44–46] Surprisingly, in the present case, the only product isolated upon reaction of $(E)/(Z)$-**1** or $(E,E)/(Z,E)$-**2** with ^{1}O$_2$ followed by purification on column chromatography (SiO$_2$ or neutral Al$_2$O$_3$) was benzophenone (**5**), regardless of the solvent used. Worthy of note was that (E)-**1** and (E,E)-**2** isomers reacted faster than (Z)-**1** and (Z,E)-**2**, respectively, which was attributed to the ability of (E)-**1** and (E,E)-**2** to more easily adopt the s-*cis* conformation for the [4+2] cycloaddition of ^{1}O$_2$.

    Scheme 3 outlines the possible reaction pathways 1–4 for the ^{1}O$_2$ photooxygenation of $(E)/(Z)$-**1** and $(E,E)/(Z,E)$-**2**; pathways 1 and 4 should be *a priori* favored by resonance stabilization of the initially formed biradical or zwitterionic species. In pathways 1 and 3, ^{1}O$_2$ is added to C(1) or C(3), respectively, to afford the corresponding open, biradical or dipolar intermediates. These intermediates should ring-close to endoperoxide **6** or dioxetanes **7** and **8**, which are often known to be thermally labile compounds, and should rapidly degrade into aldehydes **9** and **10**, and other secondary oxygenated products. In a similar fashion, when ^{1}O$_2$ is added to C(2) or C(4) (Scheme 3, pathways 2 and 4, respectively), the initially formed, open biradical or dipolar intermediates should initially rearrange to intermediates **11** and **12**, which, in turn, should quickly degrade to benzophenone and other oxygenated products. Since *gem*-

diphenylcyclopropyl-substituted aldehydes **9** and **10** and further oxygenation or degradation products thereof were not detected upon photooxygenation of (*E*)/(*Z*)-**1** and (*E,E*)/(*Z,E*)-**2**, mechanistic pathways 1 and 3 were excluded. The detection of benzophenone (**5**), the formation of which is attributed to decomposition of the initially formed ring-opened (rearranged) products, clearly supports the presence of an open biradical or dipolar intermediate during the [4+2] cycloaddition of $^1O_2$ with (*E*)/(*Z*)-**1** and (*E,E*)/(*Z,E*)-**2** (Scheme 3, pathways 2 and 4).
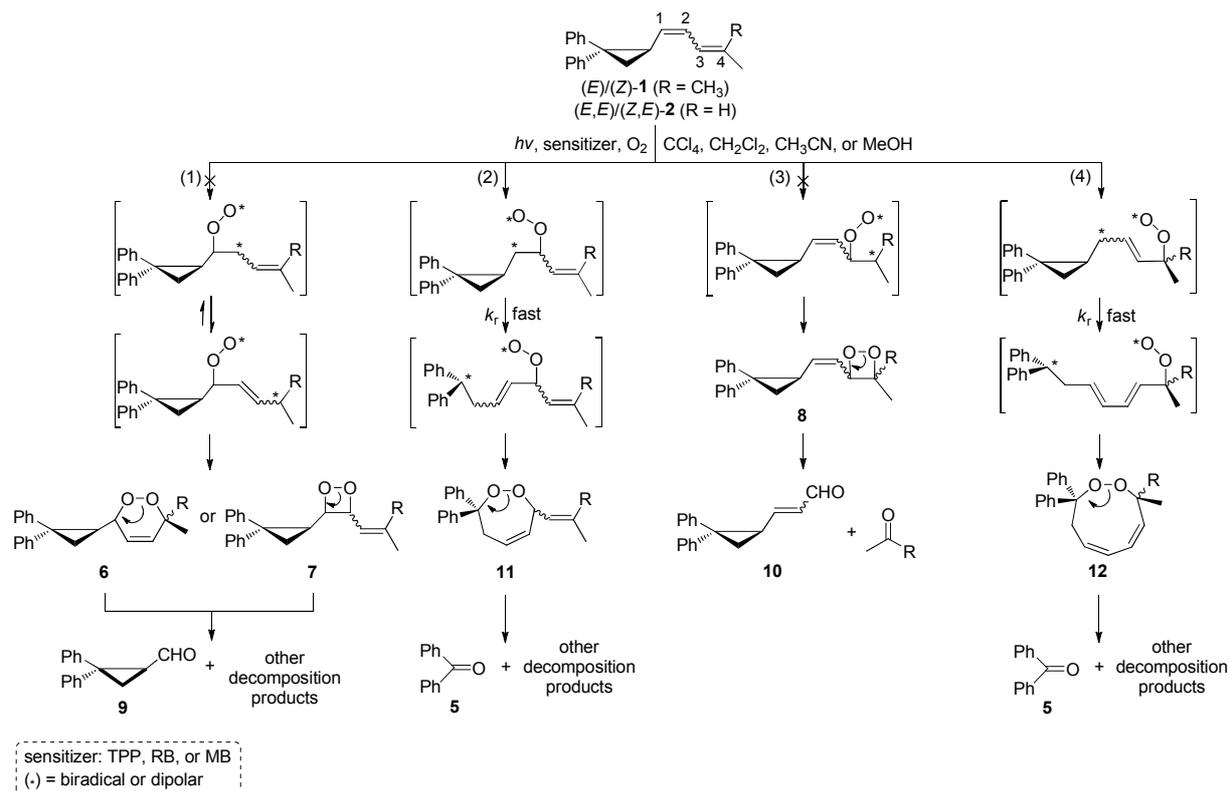
Scheme 3. Possible mechanistic pathways for the [4+2] cycloaddition of $^1O_2$ with *gem*-diphenyl-cyclopropyl-substituted 1,3-dienes (*E*)/(*Z*)-**1** and (*E,E*)/(*Z,E*)-**2**.[43] The numbering of vinyl-C-atoms follows the numbering system introduced in Scheme 2a. MB = methylene blue; RB = rose bengal; TPP = tetraphenylporphyrin.

Our next goal was to trap the initially formed endoperoxides depicted in Scheme 3, by exploiting the capability of some chemical agents (*e.g.*, PPh$_3$, Et$_3$N, and thiourea) to transform endoperoxides into stable, isolable derivatives.[15] For example, the reaction of PPh$_3$ with endoperoxides affords stable epoxy olefins.[47,48] In the present case, the photooxygenation of (*E*)/(*Z*)-**1** in CH$_2$Cl$_2$ at –40 °C followed by addition of PPh$_3$ (1.1 equiv) afforded a product which was too unstable to be isolated and structurally characterized. We further performed the photooxygenation of (*E*)/(*Z*)-**1** in CCl$_4$ at 0 °C in the presence of catalytic amount of Et$_3$N, which was expected to facilitate the rearrangement of intermediate endoperoxides into the

corresponding γ-hydroxyenones *via* the Kornblum DeLaMare rearrangement.[49] However, the only isolated product obtained from this reaction was again benzophenone (**5**). In a final attempt to trap any involved endoperoxide intermediate, we performed the photooxygenation of dienes (*E*)/(*Z*)-**1** and (*E,E*)/(*Z,E*)-**2**, in MeOH at 0 °C, in the presence of a mild reducing agent such as thiourea (1.1 equiv), and methylene blue (MB) as photosensitizer; endoperoxides can be reduced by thiourea to give 2-ene-1,4-diols.[15] In contrast to our initial expectations, the photooxygenation of (*E*)/(*Z*)-**1** and (*E,E*)/(*Z,E*)-**2** afforded (*E*)-**13** and (*E,E*)-**14**, respectively, as major products (Scheme 4).[50] Control experiments in the absence of either thiourea or MB showed that both components were essential for this reaction to take place. The structure of (*E*)-**13** and (*E,E*)-**14** was elucidated by NMR spectroscopic studies, including ^{1}H, ^{13}C, COSY, DEPT 135, HMQC and HMBC experiments (see Supporting Information). The value of the coupling constants between the vicinal vinylic protons ($^3J_{HH}$ 15.0 Hz; Scheme 4) across the C=C bonds of (*E*)-**13** and (*E,E*)-**14** is consistent with a *trans* configuration about their double bonds. In the case of (*E,E*)-**14**, this assignment was further corroborated by NOE (Scheme 4; see also Figure S9 in Supporting Information) and ^{1}H NMR decoupling experiments. Scheme 4 depicts also the ^{13}C chemical shifts (δ, ppm) of (*E,E*)-**14**. Product (*E*)-**13** showed similar spectroscopic data to that of (*E,E*)-**14** (see Experimental Section and Supporting Information).
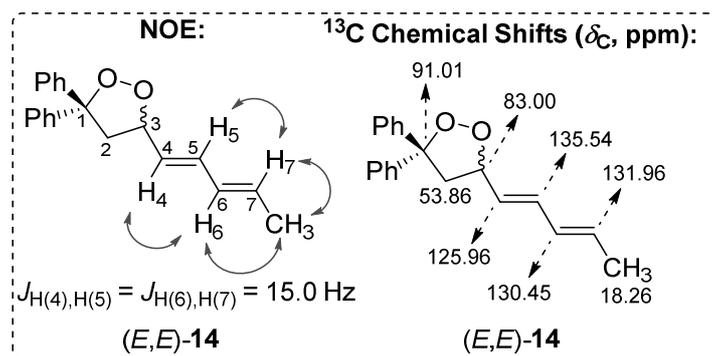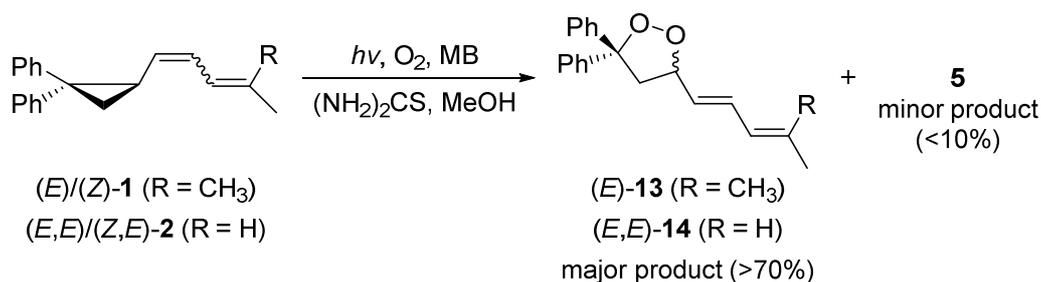
Scheme 4. Reaction of (*E*)/(*Z*)-**1** and (*E,E*)/(*Z,E*)-**2** with O$_2$ under photoinduced electron transfer conditions, in the presence of MB and thiourea, in MeOH.[43] The inset shows the key NOE correlations in product (*E,E*)-**14** (CDCl$_3$, 25 °C, 500 MHz), and its ^{13}C chemical shifts (δ, ppm; CDCl$_3$, 25 °C, 500 MHz). The inset also shows the general numbering system adopted in the present work for identifying the relevant C and H atoms of (*E*)-**13** and (*E,E*)-**14** (see also Figure

1; these numbers do not refer to the numbering system used in the systematic naming of the molecules). MB = methylene blue.

Additional evidence for the proposed structures of (*E*)-**13** and (*E,E*)-**14** was obtained from the correlation between the DFT-calculated (δ_{calcd}, reported in ppm) and experimental (δ_{expt}, reported in ppm) ^{1}H and ^{13}C NMR chemical shifts (Table 1). NMR calculations were carried out at the B3LYP/6-311+G(2d,p)//M06-2X/6-31+G(d,p) level of theory using the gauge-including atomic orbital (GIAO) method in chloroform (using the IEFPCM solvation model).[51] A typical procedure included the identification of low-energy conformational isomers of (*E*)-**13** and (*E,E*)-**14** (Figure 1; see also Figures S12–S13 in Supporting Information), followed by calculations of free energies and NMR shielding tensors (σ, in ppm) for each structure resulting from the conformational search. The computed set of isotropic magnetic shielding tensor values (σ_{iso}, in ppm) for each nucleus in all conformers were scaled, referenced, and averaged (using the mole fraction of each conformation), to generate a set of Boltzmann-weighted average chemical shifts (δ_{calcd}, in ppm; Table 1).[51] The mean absolute errors (MAEs) between the experimental and computed chemical shifts associated with the ^{1}H and ^{13}C nuclei of the structures (*E*)-**13** and (*E,E*)-**14** are given in the last row of Table 1. A perusal of this data clearly indicates a good agreement between the experimental and the computed ^{1}H and ^{13}C chemical shifts (δ_{expt} *vs* δ_{calcd}), which further supports the assigned structures of (*E*)-**13** and (*E,E*)-**14**. Full details on the computational methods, as well as the optimized geometries and energies of all four conformers of (*E*)-**13** and (*E,E*)-**14** are provided in the Experimental Section and the Supporting Information, respectively. It should be noted that only one enantiomer, the one having (*S*)-configuration at C(3), was considered in our computational NMR studies.
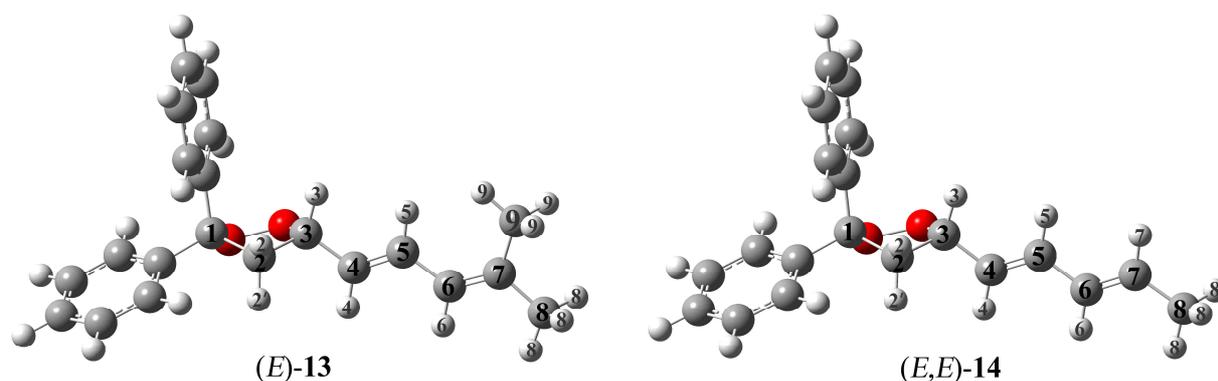
Figure 1. Structures of the lowest energy, and hence the most highly populated, conformers of (*E*)-**13** (left) and (*E,E*)-**14** (right) optimized at the M06-2X/6-31+G(d,p)/IEFPCM(chloroform) level of theory, showing the numbering system adopted in the present work for identifying the relevant C and H atoms (these numbers do not refer to the numbering system used in the systematic naming of the molecules). Color code: white = H; gray = C; red = O. The structures, energies, and Boltzmann populations of all four conformers considered in our GIAO NMR calculations are provided in the Supporting Information.

Table 1. Calculated [δ_{calcd}, in ppm; B3LYP/6-311+G(2d,p)//M06-2X/6-31+G(d,p)] and experimental (δ_{expt}, in ppm) ^{1}H and ^{13}C chemical shift values of (*E*)-**13** and (*E,E*)-**14** in chloroform

(*E*)-**13**						(*E,E*)-**14**					
Atom[a]	δ_{expt}[b]	δ_{calcd}[c]	Atom[a]	δ_{expt}[d]	δ_{calcd}[e]	Atom[a]	δ_{expt}[b]	δ_{calcd}[c]	Atom[a]	δ_{expt}[b]	δ_{calcd}[e]
C(1)	91.0	89.7				C(1)	91.0	89.6			
C(2)	54.0	51.8	H(2)	3.44	3.19	C(2)	53.9	51.6	H(2)	3.45	3.14
			H(2')	3.09	2.87				H(2')	3.07	2.89
C(3)	83.3	81.0	H(3)	4.88	4.31	C(3)	83.0	81.0	H(3)	4.84	4.22
C(4)	125.6	126.4	H(4)	5.43	5.58	C(4)	126.0	126.8	H(4)	5.45	5.58
C(5)	132.0	128.8	H(5)	6.45	6.50	C(5)	135.5	133.6	H(5)	6.21	6.12
C(6)	124.1	121.9	H(6)	5.79	5.88	C(6)	130.4	129.1	H(6)	6.01	6.17
C(7)	138.2	141.3				C(7)	132.0	133.4	H(7)	5.73	5.84
C(8)	26.2	25.0	H(8)	1.76	1.79	C(8)	18.3	18.0	H(8)	1.74	1.79
C(9)	18.5	16.6	H(9)	1.72	1.76						
MAE[f]=2.02			**MAE[f]=0.17**			**MAE[f]=1.42**			**MAE[f]=0.21**		

[a] All atoms are numbered according to the numbering system introduced in Figure 1. [b] NMR spectra were recorded on a 500 MHz spectrometer, in CDCl$_3$ at 25 °C. [c] Chemical shifts were derived from application of scaling factors (slope = −1.0522, intercept = 181.2412)[51] to the ^{13}C NMR shielding tensors computed at the B3LYP/6-311+G(2d,p)//M06-2X/6-31+G(d,p) level of theory, followed by Boltzmann averaging over all four conformers at 298 K (further details are provided in the Experimental Section). [d] ^{1}H NMR spectrum was recorded on a 300 MHz spectrometer, in CDCl$_3$ at 25 °C. [e] Chemical shifts were derived from application of scaling factors (slope = −1.0767, intercept = 31.9477)[51] to the ^{1}H NMR shielding tensors computed at the B3LYP/6-311+G(2d,p)//M06-2X/6-31+G(d,p) level of theory, followed by Boltzmann averaging over all four conformers at 298 K (further details are provided in the Experimental Section). [f] MAE is defined as the sum of the absolute errors ($\Sigma |\delta_{calcd} - \delta_{expt}|$) divided by the total number (*n*) of chemical shifts values included in the comparison; MAE=$\Sigma |\delta_{calcd} - \delta_{expt}|/n$.

It is known that the radical-mediated addition of molecular oxygen to substituted vinylcyclopropanes affords the corresponding 1,2-dioxolanes,[52] and that the co-sensitized photo-oxygenation of 1,1-diphenyl-2-vinylcyclopropane in the presence of 9,10-dicyanoanthracene (DCA) and biphenyl (BP), affords the corresponding 1,2-dioxolane as a major product *via* an electron transfer (ET) mechanism.[53] On the other hand, the formation of 1,2-dioxolanes in the presence of thiourea and MB has not been reported, though MB is known to react *via* an ET mechanism or *via* a Type I mechanism.[54] Hence, based on the above, we presume that such an ET mechanism is also operating in the present case. Specifically, the mechanism should be initiated by excitation of the photosensitizer to its singlet excited state ([1]MB[*]), which decays *via* intersystem crossing (ISC) to its triplet excited state ([3]MB[*]), followed by ET from thiourea (T) to

[3]MB[*], thus forming the corresponding geminate radical ion pair (Scheme 5). The incipient radical anion MB[•−] reacts with molecular oxygen to form superoxide radical anion ($O_2^{•-}$), while the geminal radical cation (T[•+]) oxidizes the *gem*-diphenylcyclopropyl-substituted diene. The incipient radical cation of this diene undergoes a facile ring opening of the cyclopropane ring before combining with $O_2^{•-}$ to afford, after ring closure, the corresponding 1,2-dioxolanes.
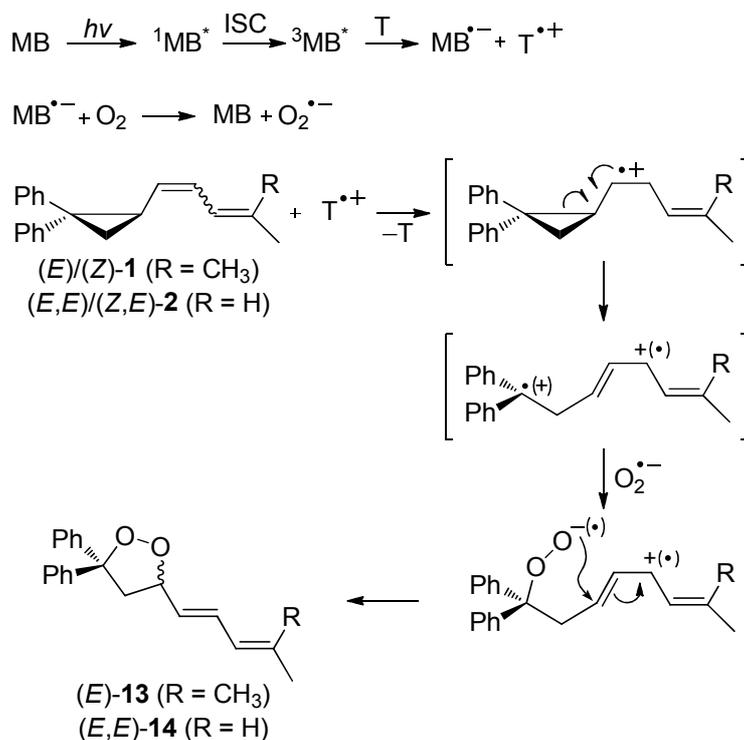
Scheme 5. Proposed reaction mechanism for the photooxygenation of (*E*)/(*Z*)-**1** and (*E,E*)/(*Z,E*)-**2** *via* photochemical co-sensitized ET.[43] ET = electron transfer, ISC = intersystem crossing, MB = methylene blue, T = thiourea.

Conclusions

gem-Diphenylcyclopropyl-substituted 1,3-dienes (*E*)/(*Z*)-**1** and (*E,E*)/(*Z,E*)-**2** were used as mechanistic probes for the investigation of the [4+2] cycloaddition of $^1O_2$, in solvents of varying polarity and proton donating ability (CCl_4, CH_2Cl_2, CH_3CN, and MeOH). In all cases, benzophenone, a decomposition product of the proposed endoperoxide intermediate **11** or **12**, was identified as the major product, whereas adducts that bear an intact cyclopropyl ring were not detected. These results provide strong evidence for the involvement of an open biradical or dipolar intermediate with a lifetime greater than 2 psec. Attempts to further trap any endo-peroxide intermediate involved in the reaction mechanism, revealed another interesting mode of

reactivity of these dienic substrates, wherein the corresponding 1,2-dioxolane derivatives (*E*)-**13** and (*E,E*)-**14** were produced *via* a co-sensitized ET mechanism, in the presence of MB and thiourea. The structures of (*E*)-**13** and (*E,E*)-**14** were supported by both experimental and theoretical NMR investigations. Further studies to explore this transformation are currently in progress in our laboratory.

Experimental Section

General. Reagents and solvents were purchased in reagent grade quality from Fluka, Merck, and Sigma-Aldrich and used without further purification. The chromatographic separations were carried out either on SiO_2 60 (particle size 0.040–0.063 mm, 230–400 mesh; Silicycle) or on Al_2O_3 (Alumina N, Act. III; EcoChrom). Flash column chromatography (FC) was carried out by applying an overpressure of 0.1–0.6 bar. Thin-layer chromatography (TLC) was conducted on SiO_2-layered aluminium plates (60 F_{254}, Merck); visualization with a UV lamp (254 or 366 nm) and/or by staining with $KMnO_4$ solution (0.5% in 1 M aqueous NaOH solution). Evaporation *in vacuo* was performed at 45–60 °C and 900–10 mbar. Drying was performed *in vacuo* at 10^{-2} Torr. ^1H and ^{13}C NMR spectra were recorded at 500 or 300 and 125 or 75 MHz, respectively on a BRUKER AMX-500 or MSL-300 instrument. Chemical shifts (δ) are reported in ppm downfield from tetramethylsilane using the residual deuterated solvent signals as an internal reference ($CDCl_3$: δ_H = 7.26 ppm, δ_C = 77.16 ppm). For ^1H NMR, coupling constants *J* are given in Hz and the resonance multiplicity is described as s (singlet), d (doublet), t (triplet), m (multiplet), and br (broad). All spectra were recorded at 25 °C. The H and C atom numbering is defined in the structures shown in Figure 1. Infrared (IR) spectra were recorded on a Perkin-Elmer 1600 FT-IR spectrometer (ATR, Golden Gate) and are reported as wavenumbers $\tilde{\nu}$ (cm^{-1}) with band intensities indicated as vs (very strong), s (strong), m (medium), and w (weak). Mass spectra were recorded on a Shimadzu GCMS-QP5050A apparatus equipped with a 50 m HP-5 capillary column and a 5971A MS detector. High-resolution (HR) EI-MS spectra were measured on a Waters Micromass AutoSpec-Ultima spectrometer, and HR-FT-ICR-MALDI-MS spectra were measured on a Varian IonSpec Fourier Transform (FT) ICR instrument with ([(2*E*)-3-[4-(*tert*-butyl)phenyl]-2-methylprop-2-enylidene]malononitrile) (DCTB) as matrix. Nomenclature follows the suggestions proposed by ACD/Labs' nomenclature software ACD/Name. The atoms were labelled arbitrarily, if necessary.

gem-Diphenylcyclopropyl-substituted 1,3-dienes 1,1'-{2-[(1*E*/1*Z*)-4-methyl-1,3-pentadien-1-yl]-1,1-cyclopropanediyl}dibenzene [(*E*)/(*Z*)-**1**; *E/Z* = 30/70] and 1,1'-{2-[(1*E*,3*E*/1*Z*,3*E*)-1,3-pentadien-1-yl]-1,1-cyclopropanediyl}dibenzene [(*E,E*)/(*Z,E*)-**2**; (*E,E*)/(*Z,E*) = 35/65] were prepared according to our previously reported procedure.[39] Both compounds represent mixtures of stereoisomers, which were used without further separation.[43]

Photooxygenations of (*E*)/(*Z*)-1 and (*E,E*)/(*Z,E*)-2. General procedure. A solution of diene (10–15 mg) in CCl$_4$ (15–20 mL) containing a catalytic amount of *meso*-tertaphenylporphyrin (TPP) as sensitizer (10^{-4} M) was bubbled gently with oxygen and irradiated with a 300 W Xenon lamp for 30 min at 0 ^{o}C. Similar procedure was followed when CH$_2$Cl$_2$ (at –78, –40 or 0 ^{o}C, using TPP as sensitizer), CH$_3$CN (at –40 or 0 ^{o}C, using RB as sensitizer) or MeOH (at –78, –40 or 0 ^{o}C, using MB as sensitizer) was used as solvent. Owing to the small solubility of dienes (*E*)/(*Z*)-**1** and (*E,E*)/(*Z,E*)-**2** in MeOH, a trace amount of CH$_2$Cl$_2$ was added to the reaction mixture. All reactions were monitored by ^{1}H NMR. The irradiation time was varied from 30 min to 1 h. The reaction mixture was concentrated *in vacuo*. Purification by FC (SiO$_2$; hexanes/EtOAc, 9:1, v/v, with 1% Et$_3$N) afforded benzophenone (**5**) as a colorless solid (45%). It should be noted that when CCl$_4$ was used as a solvent, a small amount of an unidentified side product was detected (<5%). The identity of **5** was confirmed by comparison with a commercial sample. R_f = 0.29 (SiO$_2$; hexanes/EtOAc 9:1); mp 49 ^{o}C; IR (neat): $\tilde{\nu}$ = 3287 (w), 3087 (w), 3055 (w), 3002 (w), 1981 (w), 1648 (s), 1628 (m), 1592 (m), 1574 (m), 1560 (m), 1508 (w), 1499 (w), 1447 (m), 1318 (m), 1275 (s), 1175 (w), 1160 (w), 1150 (w), 1076 (w), 1028 (w), 999 (w), 971 (w), 944 (m), 936 (m), 917 (m), 865 (w), 812 (m), 764 (m), 720 (w), 700 (s), 691 (vs), 636 (s) cm^{-1}; ^{1}H NMR (CDCl$_3$, 500 MHz, 25 ^{o}C): δ_H 7.49 (4H, br. t, $^3J_{HH}$ 7.7 Hz), 7.59 (2H, m), 7.81 (4H, d, $^3J_{HH}$ 7.2 Hz) ppm; ^{13}C NMR (CDCl$_3$, 75 MHz, 25 ^{o}C): δ_C 128.4, 130.1, 132.5, 137.7, 196.8 ppm; MS: *m/z* (%): 182 (41), 105 (100), 77 (62), 51 (25).

Photooxygenations of (*E*)/(*Z*)-1 and (*E,E*)/(*Z,E*)-2 in the presence of PPh$_3$. A solution of (*E*)/(*Z*)-**1** (10 mg, 0.04 mmol) in CH$_2$Cl$_2$ (10 mL) containing a catalytic amount of TPP as sensitizer (10^{-4} M) was bubbled gently with oxygen and irradiated with a 300 W Xenon lamp for 1 h at –40 ^{o}C. After warming at ambient temperature, PPh$_3$ (12 mg, 0.04 mmol) was added and the reaction mixture was stirred for 1 h. Subsequently, the solution was concentrated *in vacuo* to afford a product that was too unstable to be purified and structurally characterized.

Photooxygenations of (*E*)/(*Z*)-1 and (*E,E*)/(*Z,E*)-2 in the presence of Et$_3$N. A solution of diene (10 mg, 0.04 mmol) and Et$_3$N (0.01 mmol, 1 μL) in CCl$_4$ (10 mL) containing a catalytic amount of TPP as sensitizer (10^{-4} M) was bubbled gently with oxygen and irradiated with a 300 W Xenon lamp for 30 min at 0 ^{o}C. After warming at ambient temperature, the reaction mixture was concentrated *in vacuo*. Purification by FC (SiO$_2$; hexanes/EtOAc, 9:1, v/v, with 1% Et$_3$N) afforded **5** as a colorless solid.

Photooxygenations of (*E*)/(*Z*)-1 and (*E,E*)/(*Z,E*)-2 in the presence of (NH$_2$)$_2$CS. A solution of (*E*)/(*Z*)-**1** (10 mg, 0.04 mmol) and (NH$_2$)$_2$CS (3 mg, 0.04 mmol) in MeOH (15 mL) containing a catalytic amount of MB as sensitizer (10^{-4} M) was bubbled gently with oxygen and irradiated with a 300 W Xenon lamp for 1 h at 0 ^{o}C. Note that due to the small solubility of diene (*E*)/(*Z*)-**1** in MeOH, a trace amount of CH$_2$Cl$_2$ was added to the reaction mixture. After warming at ambient temperature, the reaction mixture was concentrated *in vacuo*. Purification by FC (SiO$_2$; hexanes/EtOAc, 9:1, v/v) afforded 1,2-dioxolane (*E*)-**13** (8 mg, 72%) as a pale yellow solid. Photooxygenation of (*E,E*)/(*Z,E*)-**2** was performed in a similar manner affording 1,2-dioxolane (*E,E*)-**14** (8 mg, 74%) as a pale yellow solid.

5-[(1E)-4-Methyl-1,3-pentadien-1-yl]-3,3-diphenyl-1,2-dioxolane [(E)-13]: R_f = 0.34 (SiO$_2$; hexanes/EtOAc 9:1); mp >80 °C (decomp); IR (neat): $\tilde{\nu}$ = 3054 (w), 3018 (w), 2927 (m), 2854 (w), 1720 (w), 1691 (w), 1659 (m), 1598 (w), 1492 (m), 1447 (s), 1377 (w), 1317 (w), 1277 (w), 1178 (w), 1151 (w), 1075 (s), 1028 (s), 971 (m), 941 (w), 918 (m), 809 (w), 750 (s), 697 (m), 638 (m) cm^{-1}; ^{1}H NMR (CDCl$_3$, 500 MHz, 25 °C): δ_H 1.72 (s, 3 H; 3 H-9), 1.76 (s, 3 H; 3 H-8), 3.09 (dd, $^3J_{HH}$ 7.0, 12.2 Hz, 1 H; H-2'), 3.44 (dd, $^3J_{HH}$ 7.0, 12.2 Hz; 1 H; H-2), 4.88 (m, 1 H; H-3), 5.43 (dd, $^3J_{HH}$ 8.4, 15.0 Hz, 1 H; H-4), 5.79 (d, $^3J_{HH}$ 11.0 Hz, 1 H; H-6), 6.45 (dd, $^3J_{HH}$ 11.0, 15.0 Hz, 1 H; H-5), 7.24–7.46 (m; 10 H; arom. H) ppm; ^{13}C NMR (CDCl$_3$, 75 MHz, 25 °C): δ_C 18.5 (C-9), 26.2 (C-8), 54.0 (C-2), 83.3 (C-3), 91.0 (C-1), 124.1 (C-6), 125.6 (C-4), 126.5, 126.7, 127.7, 128.4, 128.5, 130.2, 132.0 (C-5), 138.2 (C-7), 142.8, 143.0 ppm; HR-EI-MS: m/z (%): 182.0722 (56, [Ph$_2$C=O]$^+$, calcd for C$_{13}$H$_{10}$O$^+$: 182.0726), 105.0339 (100, [PhC=O]$^+$, calcd for C$_7$H$_5$O$^+$: 105.0335), 77.0388 (36, C$_6$H$_5$$^+$, calcd for C$_6H_5$$^+$: 77.0386); HR-MALDI-MS (DCTB): m/z (%): 306.1488 (23, M^+, calcd for C$_{21}$H$_{22}$O$_2$$^+$: 306.1620), 305.1455 (100, [M – H]$^+$, calcd for C$_{21}$H$_{21}$O$_2$$^+$: 305.1536).

5-[(1E,3E)-1,3-Pentadien-1-yl]-3,3-diphenyl-1,2-dioxolane [(E,E)-14]: R_f = 0.31 (SiO$_2$; hexanes/EtOAc 9:1); mp >80 °C (decomp); IR (neat): $\tilde{\nu}$ = 3054 (w), 3018 (w), 2968 (m), 2927 (w), 1718 (w), 1689 (w), 1657 (m), 1598 (w), 1577 (w), 1492 (m), 1447 (s), 1369 (w), 1318 (w), 1277 (m), 1174 (w), 1155 (w), 1060 (w), 1027 (m), 1001 (m), 971 (m), 941 (w), 918 (m), 856 (w), 804 (w), 749 (s), 696 (m), 663 (w), 638 (m) cm^{-1}; ^{1}H NMR (CDCl$_3$, 500 MHz, 25 °C): δ_H 1.74 (d, $^3J_{HH}$ 6.5 Hz, 3 H; 3 H-8), 3.07 (dd, $^3J_{HH}$ 7.0, 12.0 Hz, 1 H; H-2'), 3.45 (dd, 1H, $^3J_{HH}$ 7.0, 12.0 Hz, 1 H; H-2), 4.84 (m, 1 H; H-3), 5.45 (dd, $^3J_{HH}$ 10.0, 15.0 Hz, 1 H; H-4), 5.73 (m, 1 H; H-7), 6.01 (dd, $^3J_{HH}$ 12.0, 15.0 Hz, 1 H; H-6), 6.21 (dd, $^3J_{HH}$ 10.0, 15.0 Hz, 1 H; H-5), 7.26–7.45 (m, 10 H; arom. H) ppm; ^{13}C NMR (CDCl$_3$, 125 MHz, 25 °C): δ_C 18.3 (C-8), 53.9 (C-2), 83.0 (C-3), 91.0 (C-1), 126.0 (C-4), 126.5, 126.7, 127.7, 128.50, 128.51, 130.4 (C-6), 132.0 (C-7), 135.5 (C-5), 142.7, 142.9 ppm; HR-EI-MS: m/z (%): 292.0942 (1, M^+, calcd. for C$_{20}$H$_{20}$O$_2$$^+$: 292.1463), 182.0727 (51, [Ph$_2$C=O]$^+$, calcd for C$_{13}$H$_{10}$O$^+$: 182.0726), 105.0337 (100, [PhC=O]$^+$, calcd for C$_7$H$_5$O$^+$: 105.0335), 77.0390 (30, C$_6$H$_5$$^+$, calcd for C$_6H_5$$^+$: 77.0386).

Computational methods. The minimum energy conformations for each compound [(E)-**13** and (E,E)-**14**] were identified using a Molecular Mechanics conformational search with the MMFF force field as implemented in Spartan 08 software package,[55] using a starting geometry with (S) absolute configuration on the C-3 stereocenter (Figure 1). A set of four low-energy conformers with relative energies within a 10 kJ mol^{-1} window were identified for each of the two 1,2-dioxolanes [(E)-**13** and (E,E)-**14**]. The energies and optimal geometries of all conformers were then determined at a higher level of theory, using the M06-2X density functional with the 6-31+G(d,p) basis set, and implicit solvation in CHCl$_3$ (IEFPCM; integral equation formalism variant of the polarizable continuum model), as implemented in Gaussian 09 software package (Revision A.02).[56] Solute cavities were constructed using default united-atom radii (UA0). A pruned (99,590) integration grid (99 radial shells and 590 angular points per shell; *ultrafine* grid in Gaussian 09) and very tight geometrical convergence criteria were employed. All

optimized structures were verified as ground-state minima by performing frequency calculations at the same level of theory (no imaginary frequencies were found), the data from which were also used to compute their Boltzmann distribution at 298 K. The first most stable conformers of (*E*)-**13** and (*E,E*)-**14**, accounting for overall 82.3% and 90.0% population, respectively, at 298 K, are shown in Figure 1, while all four low-energy conformers of each compound are shown in Figures S12–S13 in the Supporting Information. All optimized structures were then used for NMR calculations. NMR shielding tensors (σ, in ppm) were computed with the gauge-independent atomic orbitals (GIAO) method at the B3LYP/6-311+G(2d,p) level of theory, including chloroform solvation effects (using the IEFPCM solvation model), while employing solute cavities built from Bondi radii as implemented in Gaussian 09. A pruned (99,590) integration grid was employed. The computed isotropic magnetic shielding tensors (σ_{iso}, in ppm) for each nucleus in all conformers was converted to referenced and empirically scaled chemical shifts (δ_{scaled}, in ppm) by applying scaling and referencing factors (slope and intercept, respectively) according to the equation: $\delta_{scaled} = (\sigma_{iso} - \text{intercept}) / \text{slope}$, where δ_{scaled} is the referenced/scaled chemical shift (in ppm), and σ_{iso} is the isotropic computed NMR shielding tensor (in ppm). The slope and intercept values are typically obtained by linear regression analysis of a plot of the calculated isotropic magnetic shielding tensors (σ_{iso}) against the corresponding experimental chemical shifts (δ_{expt}). In the present study, we used generic-scaling factors obtained from large datasets [*i.e.* obtained from linear regression analysis of a plot of calculated isotropic magnetic shielding tensors (σ_{iso}) against experimental chemical shifts (δ_{expt}) of a large series of compounds]; these scaling/referencing factors are specific of the level of theory used. For the level of theory used herein [B3LYP/6-311+G(2d,p)//M06-2X/6-31+G(d,p)] the following values have been calculated by Willoughby *et al.*,[51]: for [1]H: intercept = 31.9477, slope = –1.0767; for [13]C: intercept = 181.2412, slope = –1.0522. The final calculated chemical shift values (δ_{calcd}, in ppm; Table 1) were determined by Boltzmann averaging the scaled chemical shift values (δ_{scaled}, in ppm), based on the calculated Gibbs free energy values of each conformer. Specifically, by using the free energy data (kcal mol^{-1}) obtained from the frequency calculations, a Boltzmann weighting factor [$e^{(-E/RT)}$, where E is the relative energy (kcal mol^{-1}) with respect to the most stable conformer, T is the temperature (in K), and R is the gas constant (0.001986 kcal mol^{-1} K^{-1})] was determined for each conformer at 298 K, which was, in turn, converted into the relative mole fraction by dividing the calculated Boltzmann factor of each conformer by the sum of all the Boltzmann factors of all contributing conformers. The resulting weighting factors (mole fraction contributions) were applied to the scaled chemical shift values (δ_{scaled}, in ppm) for each nucleus of each individual conformer. Summation of the weighted chemical shifts across all conformers generates the final Boltzmann-weighted average chemical shifts (δ_{calcd}, in ppm) used to compare against experimental data (δ_{expt}, in ppm; Table 1). The computed ^{1}H chemical shifts of each methyl group were arithmetically averaged due to their conformational freedom (*i.e.* free rotation at 298 K), while the calculated chemical shifts of the H and C atoms of the two phenyl rings were not included in the comparison, since the corresponding experimental chemical shifts could not be unambiguously assigned (however, it

should be noted that comparison of all chemical shifts data –including tentatively assigned experimental chemical shifts for the phenyl H and C atoms– was again in very good agreement with the calculated values).

Supplementary Material

Copies of NMR spectra of (*E*)-**13** (^{1}H NMR, ^{13}C NMR, COSY, HMQC) and (*E,E*)-**14** (^{1}H NMR, ^{13}C NMR, DEPT 135, COSY, NOE, HMBC, HMQC); optimized geometries (in Cartesian coordinates), total energies, relative free energies, and Boltzmann populations of all contributing conformers of (*E*)-**13** and (*E,E*)-**14**.

Acknowledgements

References

1. Frimer, A. A. *Singlet Oxygen*; CRC Press: Boca Raton, FL, 1985; Vol. 1–4.
2. Foote, C. S.; Clennan, E. L. in *Active Oxygen in Chemistry*; Foote, C. S.; Valentine, J. S.; Greenberg, A.; Liebman, J. F. Eds.; Chapman & Hall: London, 1995; pp 105–140.
3. Clennan, E. L.; Pace, A. *Tetrahedron* **2005**, *61*, 6665–6691.
   http://dx.doi.org/10.1016/j.tet.2005.04.017
4. DeRosa, M. C.; Crutchley, R. J. *Coord. Chem. Rev.* **2002**, *233–234*, 351–371, and references cited therein.
   http://dx.doi.org/10.1016/S0010-8545(02)00034-6
5. Ogilby, P. R. *Chem. Soc. Rev.* **2010**, *39*, 3181–3209, and references cited therein.
   http://dx.doi.org/10.1039/B926014P
6. Montagnon, T.; Tofi, M.; Vassilikogiannakis, G. *Acc. Chem. Res.* **2008**, *41*, 1001–1011.
   http://dx.doi.org/10.1021/ar800023v
7. Gonçalves, E. S.; Ogilby, P. R. *Langmuir* **2008**, *24*, 9056–9065, and references cited therein.
   http://dx.doi.org/10.1021/la801353n

8. Kim, H.; Kim, W.; Mackeyev, Y.; Lee, G.-S.; Kim, H.-J.; Tachikawa, T.; Hong, S.; Lee, S.; Kim, J.; Wilson, L. J.; Majima, T.; Alvarez, P. J. J.; Choi, W.; Lee, J. *Environ. Sci. Technol.* **2012**, *46*, 9606–9613.
    http://dx.doi.org/10.1021/es301775k

9. Rosado-Lausell, S. L.; Wang, H.; Gutiérrez, L.; Romero-Maraccini, O. C.; Niu, X.-Z.; Gin, K. Y. H.; Croué, J.-P.; Nguyen, T. H. *Water Res.* **2013**, *47*, 4869–4879.
    http://dx.doi.org/10.1016/j.watres.2013.05.018

10. Davies, M. J. *Biochem. Biophys. Res. Commun.* **2003**, *305*, 761–770.
    http://dx.doi.org/10.1016/S0006-291X(03)00817-9

11. Redmond, R. W.; Kochevar, I. E. *Photochem. Photobiol.* **2006**, *82*, 1178–1186.
    http://dx.doi.org/10.1562/2006-04-14-IR-874

12. Triantaphylidès, C.; Krischke, M.; Hoeberichts, F. A.; Ksas, B.; Gresser, G.; Havaux, M.; Van Breusegem, F.; Mueller, M. J. *Plant Physiol.* **2008**, *148*, 960–968.
    http://dx.doi.org/10.1104/pp.108.125690

13. Jarvi, M. T.; Niedre, M. J.; Patterson, M. S.; Wilson, B. C. *Photochem. Photobiol.* **2006**, *82*, 1198–1210.
    http://dx.doi.org/10.1562/2006-05-03-IR-891

14. Maisch, T.; Baier, J.; Franz, B.; Maier, M.; Landthaler, M.; Szeimies, R.-M.; Bäumler, W. *Proc. Natl Acad. Sci. USA* **2007**, *104*, 7223–7228.
    http://dx.doi.org/10.1073/pnas.0611328104

15. Balci, M. *Chem. Rev.* **1981**, *81*, 91–108.
    http://dx.doi.org/10.1021/cr00041a005

16. Adam, W.; Bosio, S.; Bartoschek A.; Griesbeck, A. G. *"Photooxygenation of 1,3-Dienes"* in *CRC Handbook of Organic Photochemistry and Photobiology*, 2nd Edn.; Horspool, W.; Lenci, F. Eds.; CRC Press: Boca Raton, 2004; Chapter 25, pp 25-1–25-19, and references cited therein.

17. Iesce, M. R.; Cermola, F. in *CRC Handbook of Organic Photochemistry and Photobiology*, 3rd Edn.; Griesbeck, A.; Oelgemöller, M.; Ghetti, F. Eds.; CRC Press: Boca Raton, 2012; Chapter 30.3, pp 728–749, and references cited therein.

18. Clennan, E. L. *Tetrahedron* **1991**, *47*, 1343–1382, and references cited therein.
    http://dx.doi.org/10.1016/S0040-4020(01)86413-9

19. McCarrick, M. A.; Wu, Y.-D.; Houk, K. N. *J. Org. Chem.* **1993**, *58*, 3330–3343.
    http://dx.doi.org/10.1021/jo00064a020

20. Adam, W.; Prein, M. *Acc. Chem. Res.* **1996**, *29*, 275–283.
    http://dx.doi.org/10.1021/ar950164y

21. Sevin, F; McKee, M. L. *J. Am. Chem. Soc.* **2001**, *123*, 4591–4600.
    http://dx.doi.org/10.1021/ja010138x

22. Reddy, A. R.; Bendikov, M. *Chem. Commun.* **2006**, 1179–1181.
    http://dx.doi.org/10.1039/B513597D

23. Rigaudy, J.; Capdevielle, P.; Combrisson, S.; Maumy, M. *Tetrahedron Lett.* **1974**, *15*, 2757–2760.
http://dx.doi.org/10.1016/S0040-4039(01)91733-2

24. Van den Heuvel, C. J. M.; Verhoeven, J. W.; De Boer, T. J. *Rec. Trav. Chim. Pays-Bas* **1980**, *99*, 280–284.
http://dx.doi.org/10.1002/recl.19800990908

25. Gollnick, K.; Griesbeck, A. *Tetrahedron* **1984**, *40*, 3235–3250.
http://dx.doi.org/10.1016/0040-4020(84)85006-1

26. Motoyoshiya, J.; Okuda, Y.; Matsuoka, I.; Hayashi, S.; Takaguchi, Y.; Aoyama, H. *J. Org. Chem.* **1999**, *64*, 493–497.
http://dx.doi.org/10.1021/jo981506r

27. Bobrowski, M.; Liwo, A.; Ołdziej, S.; Jeziorek, D.; Ossowski, T. *J. Am. Chem. Soc.* **2000**, *122*, 8112–8119.
http://dx.doi.org/10.1021/ja001185c

28. Chien, S.-H.; Cheng, M.-F.; Lau, K.-C.; Li, W.-K. *J. Phys. Chem. A* **2005**, *109*, 7509–7518.
http://dx.doi.org/10.1021/jp0503009

29. Dewar, M. J. S.; Thiel, W. *J. Am. Chem. Soc.* **1977**, *99*, 2338–2339.
http://dx.doi.org/10.1021/ja00449a053

30. Gollnick, K.; Griesbeck, A. *Tetrahedron Lett.* **1983**, *24*, 3303–3306.
http://dx.doi.org/10.1016/S0040-4039(00)86254-1

31. O'Shea, K. E.; Foote, C. S. *J. Am. Chem. Soc.* **1988**, *110*, 7167–7170.
http://dx.doi.org/10.1021/ja00229a035

32. Delogu, G.; Fabbri, D.; Fabris, F.; Sbrogiò, F.; Valle, G.; De Lucchi, O. *J. Chem. Soc., Chem. Commun.* **1995**, 1887–1888.
http://dx.doi.org/10.1039/C39950001887

33. Clennan, E. L.; Mehrsheikh-Mohammadi, M. E. *J. Am. Chem. Soc.* **1984**, *106*, 7112–7118, and references cited therein.
http://dx.doi.org/10.1021/ja00335a040

34. Gorman, A. A.; Hamblett, I.; Lambert, C.; Spencer, B.; Standen, M. C. *J. Am. Chem. Soc.* **1988**, *110*, 8053–8059.
http://dx.doi.org/10.1021/ja00232a016

35. Aubry, J.-M.; Mandard-Cazin, B.; Rougee, M.; Bensasson, R. V. *J. Am. Chem. Soc.* **1995**, *117*, 9159–9164.
http://dx.doi.org/10.1021/ja00141a006

36. Hatzimarinaki, M.; Roubelakis, M. M.; Orfanopoulos, M. *J. Am. Chem. Soc.* **2005**, *127*, 14182–14183.
http://dx.doi.org/10.1021/ja053431w

37. Milnes, K. K.; Jennings, M. C.; Baines, K. M. *J. Am. Chem. Soc.* **2006**, *128*, 2491–2501.
http://dx.doi.org/10.1021/ja057596g

38. Alberti, M. N.; Orfanopoulos, M. *Org. Lett.* **2008**, *10*, 2465–2468.
    http://dx.doi.org/10.1021/ol800759u
39. Alberti, M. N.; Orfanopoulos, M. *Org. Lett.* **2009**, *11*, 1659–1662.
    http://dx.doi.org/10.1021/ol900363n
40. Newcomb, M.; Glenn, A. G. *J. Am. Chem. Soc.* **1989**, *111*, 275–277.
    http://dx.doi.org/10.1021/ja00183a041
41. Newcomb, M.; Johnson, C. C.; Manek, M. B.; Varick, T. R. *J. Am. Chem. Soc.* **1992**, *114*,
    10915–10921.
    http://dx.doi.org/10.1021/ja00053a031
42. Griller, D.; Ingold, K. U. *Acc. Chem. Res.* **1980**, *13*, 317–323.
    http://dx.doi.org/10.1021/ar50153a004
43. All compounds in this paper represent mixtures of stereoisomers. In particular, taking into
    account the presence of both a cyclopropyl-C-stereocenter (*R* or *S* configuration) and a C=C
    double bond (*E* or *Z* configuration), there exist four possible stereoisomers for (*E*)/(*Z*)-**1** [*i.e.*
    (*R*,*E*); (*S*,*E*); (*R*,*Z*); and (*S*,*Z*)] and four possible stereoisomers for (*E*,*E*)/(*Z*,*E*)-**2** [*i.e.* (*R*,*E*,*E*);
    (*S*,*E*,*E*); (*R*,*Z*,*E*); and (*S*,*Z*,*E*)]. For the sake of simplicity, the '*R*' and '*S*' stereodescriptors
    have been omitted throughout this paper, and only the *R* configuration of the cyclopropyl-C-
    stereocenter in (*E*)/(*Z*)-**1** and (*E*,*E*)/(*Z*,*E*)-**2** is consistently shown throughout all schemes and
    figures.
44. Matsumoto, M.; Kuroda, K. *Synth. Commun.* **1981**, *11*, 987–992.
    http://dx.doi.org/10.1080/00397918108065759
45. Matsumoto, M.; Kuroda, K. *Tetrahedron Lett.* **1982**, *23*, 1285–1288.
    http://dx.doi.org/10.1016/S0040-4039(00)87084-7
46. Griesbeck, A. G.; Fiege, M.; Gudipati, M. S.; Wagner, R. *Eur. J. Org. Chem.* **1998**, 2833–
    2838.
    http://dx.doi.org/10.1002/(SICI)1099-0690(199812)1998:12<2833::AID-
    EJOC2833>3.0.CO;2-6
47. Adam, W.; Balci, M.; Pietrzak, B. *J. Am. Chem. Soc.* **1979**, *101*, 6285–6291.
    http://dx.doi.org/10.1021/ja00515a022
48. Adam, W.; Balci, M. *J. Org. Chem.* **1979**, *44*, 1189–1190.
    http://dx.doi.org/10.1039/C39800001062
49. Kelly, D. R.; Bansal, H.; Morgan, J. J. G. *Tetrahedron Lett.* **2002**, *43*, 9331–9333, and
    references cited therein
    http://dx.doi.org/10.1021/jo00043a007
50. The ^{1}H NMR spectra of these compounds showed the presence of minor side product(s),
    which could not be separated by flash column chromatography on silica gel (identical R_f
    values). For further details see the Supporting Information.
51. Willoughby, P. H.; Jansma, M. J.; Hoye, T. R. *Nat. Protocols* **2014**, *9*, 643–660, and
    references cited therein.
    http://dx.doi.org/10.1038/nprot.2014.042

52. Feldman, K. S. *Synlett* **1995**, 217–225, and references cited therein.
http://dx.doi.org/10.1016/0040-4039(95)01438-N

53. Shim, S. C.; Song, J. S. *J. Org. Chem.* **1986**, *51*, 2817–2818.
http://dx.doi.org/10.1021/jo00364a039

54. Manring, L. E.; Eriksen, J.; Foote, C. S. *J. Am. Chem. Soc.* **1980**, *102*, 4275–4277.
http://dx.doi.org/10.1021/ja00532a057

55. Spartan'08, Wavefunction, Inc., Irvine, CA.
http://www.wavefun.com

56. Gaussian 09, Revision A.02, M. J. Frisch, G. W. Trucks, H. B. Schlegel *et al.*, Gaussian, Inc., Wallingford CT, 2009 (The full reference for Gaussian 09 is reported in SI).
http://www.gaussian.com/